Nucleic Acid–Methylmercury(II) Interactions and the ^1H NMR Lifetimes of Nucleobase Exchangeable Protons

Do-Lan Hoo[1] and Bruce McConnell*

Contribution from the Department of Biochemistry and Biophysics, John A. Burns School of Medicine, University of Hawaii, Honolulu, Hawaii 96822.
Received November 13, 1978

Abstract: The kinetics and equilibria of methylmercury–adenine interactions were investigated by ^1H NMR three-site line-shape analysis of the 360-MHz amino proton resonances of 2′,3′-cAMP. This involved consideration of an additional mercurated species and provided both a direct demonstration of aminomercuration and a measure of the rates of the forward and reverse aminomercuration reactions, which are slow on the NMR time scale ($\sim 100\ s^{-1}$). Similar rates were obtained by two-site line-shape analysis of the nonexchanging C_2 and C_8 protons of the nucleobase, confirming the amino line-shape analysis and eliminating amino-to-water exchange mechanisms other than that associated directly with the aminomercuration as factors in amino proton line shape. These results, together with line-shape changes induced by the addition of phosphate, are consistent with a concerted four-center mechanism for aminomercuration involving direct bond formation between the nucleobase amino and methylmercuric hydroxide and water elimination. The effect of N_1-mercuration of the nucleobase is several orders of magnitude less than the effect of N_1-protonation in increasing the rates of aminomercuration and proton transfer. These conclusions are supported by preliminary results on the aminomercuration of 2′,3′-cGMP and 1-methyladenosine.

The accessibility of the amino ^1H NMR of mononucleotides in aqueous solution offers a potentially useful approach for the elucidation of metal–nucleobase binding equilibria. Owing to slow exchange, the amino proton resonance is a well-resolved signal in H_2O, whose line width is a measure of both the proton lifetime and the extent of proton interaction at the purine or pyrimidine ring.[2,3] This arises from the fact that the protonated form of the nucleobase ring site (adenine N_1, cytosine N_3, and guanine N_7) is the major kinetic intermediate for amino proton exchange in the neutral to acidic pH range.[4-6] Because the amino line broadening mechanism is known and can be expressed quantitatively (see below), changes in $-NH_2$ ^1H NMR line shape produced by a metal ion can be assigned to specific metal–nucleotide interactions. For example, direct involvement of the amino as a ligand would be seen directly and, if the purine endocyclic nitrogen were one of the ligand sites, the amino proton line width might be a measure of the metal–nucleotide dissociation constant at a pH selected to eliminate proton competition for the site. In either case an assessment of the catalysis of amino-to-water proton exchange by metal–nucleotide binding at any of the binding sites could be made. Catalysis of exchange of the guanine and inosine C_8 proton by methylmercury interaction has been demonstrated by Mansy and Tobias.[12]

This paper describes an analysis of amino ^1H NMR line shape as a method to determine the kinetics of the interaction between adenylic acid and methylmercuric hydroxide, $CH_3Hg^{II}OH$. Interest in the kinetics of methylmercury–nucleotide interaction is derived from the importance of methylmercury as a mutagen[26] and as a reagent for the limited melting of the DNA double helix.[27] The selection of $CH_3Hg^{II}OH$ is based on the similarity between CH_3Hg^+ and the proton in its general aspects[7] and in its binding to identical sites of nucleotides.[8-14] The studies of Mansy et al.[14] have confirmed earlier conclusions that the adenine N_1 is the chief CH_3Hg^+ ligand site at low pH and included evidence of proton transfer at high pH to favor a direct substitution of an amino proton by CH_3Hg^+.

The results presented in this paper include direct confirmation of aminomercuration of adenine, which establishes a slow exchange NMR domain equilibrium with the nonmercurated amino site. Calculated lifetimes of the mercurated and nonmercurated species were obtained from amino proton and nucleobase proton ^1H NMR line-shape analyses based on two-site and modified three-site exchange. Conservation of literature formation constants for the fitting of observed 360-MHz line shapes required the consideration of a mercurated species of nucleotide not encountered in related papers. The formation of the aminomercurated species is a reflection of the greater $-NH_2$ acidity of the N_1-mercurated purine, as compared to that of the free ligand. However, the amino proton exchange (acidity) of N_1-mercurated adenine is several orders of magnitude less than that of the N_1-protonated nucleotide. Because of this, aminomercuration is viewed as a four-center concerted reaction between the adenine amino and $CH_3Hg^{II}OH$, and not the result of a series of partial reactions involving the preliminary formation of CH_3Hg^+ and the amino anion.

Experimental Section

Chemicals. Nucleotides and nucleosides (Sigma) were used as supplied and weighed according to their labeled hydration weights. Methylmercury hydroxide was obtained as a gift from Morton Chemical Co. All chemicals were reagent grade.

Methylmercury(II) concentration was determined by methyl ^1H NMR chemical shift titration of the methylmercury hydroxide with thiosulfate.[15] A second analytical method, modified to detect contamination of inorganic mercury, was performed as follows: methylmercury was digested to Hg^{2+} and converted to the Hg^{2+}–dithiazone complex, which was measured at 490 nm with $HgCl_2$ as described in ref 16. To estimate both organic and inorganic mercury, 0.3 mL of stock methylmercury (0.2 M) was digested for 20 min in the presence of 0.3 g of $KMnO_4$ and 5 mL of concentrated H_2SO_4 over moderate heating in the hood. The cooled digest was brought to 500 mL with H_2O containing a small amount of $KMnO_4$. Removal of aliquots of this mixture for colorimetric Hg^{2+} determination[16] required vigorous shaking to evenly suspend the fine MnO_2 precipitate, which binds Hg^{2+}.

pH Measurement. All pH measurements were made at 25 °C with Beckman combined glass electrodes (KCl–HgCl reference) and the Beckman Research Meter or the Beckman Model 4500 meter. Possible errors in pH measurement due to mercury interaction at the reference electrode bridge were checked by the use of agar–salt bridges made according to two different procedures.[17,18] It was found that initial pH measurements with direct use of the combined electrode were accurate to ±0.05 pH when care was used to minimize exposure time to the methylmercury solutions.

^1H Nuclear Magnetic Resonance. Two NMR spectrometers were used in continuous wave mode to obtain spectra: a Varian HA-100 spectrometer of the Chemistry Department, University of Hawaii, and the Bruker HXS-360 NMR spectrometer at the Stanford Magnetic Resonance Laboratory, Stanford University.[19] The use of the latter involved accumulation and correlation of multiple fast sweeps with the use of the Nicolet 1080 computer system. Precautions to

0002-7863/79/1501-7470$01.00/0

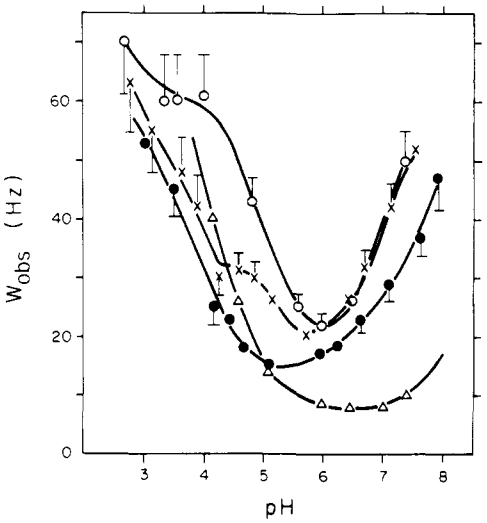

Figure 1. The effect of methylmercury on the pH dependence of the amino ^{1}H NMR 100-MHz line width of 2′,3′-cAMP. Amino proton resonances were obtained at 28 °C, 0.14 M nucleotide and 0 (△), 0.091 (●), 0.14 (×), and 0.18 M (○) methylmercuric hydroxide.

ensure independence of correlated line shape with sweep rate/filtering conditions were carried out as described previously.[6]

Calculations of species distribution for methylmercury-nucleotide species are obtained from an iterative extraction of the single real, positive root of a fourth-order polynomial between the limits of 0 and total [CH_3HgOH]. APL programs are available on request.

Results

The pronounced 100-MHz line broadening of the amino proton resonance is shown in Figure 1 as a function of pH at three ratios of [CH_3HgOH]/[2′,3′-cAMP]. Below pH 5, the low pH line broadening in the absence of methylmercury reflects increased amino-water proton exchange in response to protonation of the adenine N_1.[4] This broadening is described by

$$\pi W_{Hx} = k_{Hx} = \left(\frac{[H^+]}{K_N + [H^+]}\right) k_B[B] \qquad (1)$$

where W_{Hx} is the line broadening term in hertz, k_{Hx} is the pseudo-first-order rate constant for exchange, and k_B is the second-order rate constant for proton transfer to the conjugate base (B) of any acid-base pair.[4-6] In this case B = H_2O below pH 5. The term in parentheses expresses the mole fraction of the protonated nucleobase in terms of hydrogen ion concentration and K_N, the acid dissociation constant. Since k_B is known, the supression of line broadening in this pH region by the lowest ratio of methylmercury/nucleotide reflects a decrease in the protonated nucleobase mole fraction. This is a demonstration of (1) the competition of CH_3Hg^+ with the proton for the N_1 site and (2) a lower rate of $-NH_2$ to H_2O proton transfer (k_B of eq 1) of the N_1-mercurated adenine in comparison to that of the N_1-protonated form.[20] Higher concentrations of CH_3HgOH result in additional broadening with the appearance of a maximum seen most clearly at pH 5 for [CH_3HgOH]/[2′,3′-cAMP] = 1. Above pH 5, amino proton transfer from the neutral (free ligand) species to OH^- becomes the predominant exchange broadening mechanism in the absence of CH_3HgOH (Figure 1).[2,4] In the alkaline pH range, all ratios of CH_3HgOH/2′,3′-cAMP show extra broadening. These line-broadening features reflect mercuration reactions at the adenine N-1 and amino sites to produce amino proton resonances that remain in a slow exchange with water.

The possibility of a slow mercuration reaction at one of the two ligand sites exists as a line-broadening mechanism in addition to amino-to-water proton exchange. This is borne out by the line broadening of the nonexchanging C_2 and C_3 protons in the vicinity of pH 5 with the addition of CH_3HgOH (Figure 3). Confirmation of a slow mercuration reaction is evident with complete resolution of the C_2 and C_8 exchange doublets at 360 MHz, 3 °C, pH 6.2 (Figure 4). At this pH the concentrations of mercurated and nonmercurated species of nucleotide are approximately equal (see below). The appearance of the slowly exchanging mercurated species is seen, also, as a broad resonance forming the downfield shoulder of the amino proton

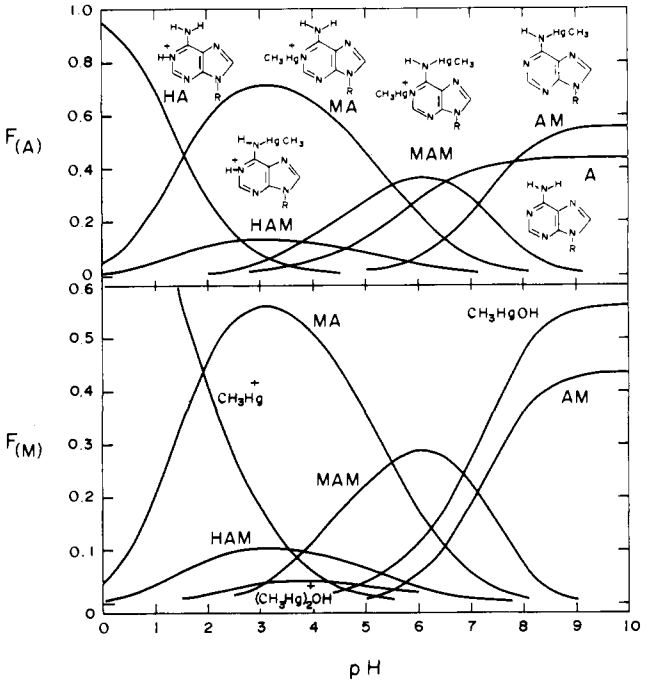

Figure 2. Calculated species distributions as a function of pH for the mixture of 2′,3′-cAMP (0.14 M) and methylmercuric hydroxide (0.18 M): (top) fraction of species relative to total nucleotide; (bottom) fraction of species relative to total methylmercury. Formation constants are listed in Table II. Abbreviations shown in top and bottom are used throughout the text. For this figure the log formation constant for reaction 7, Table II, = 3.3.

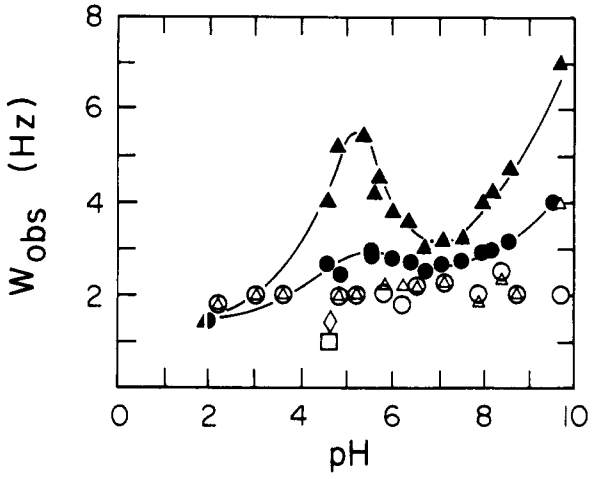

Figure 3. The pH dependence of line width of the C_2 and C_8 proton resonances of 2′,3′-cAMP in the presence of methylmercury. Line widths were measured at equal methylmercuric hydroxide and cAMP concentrations (0.14 M), from 100-MHz spectra obtained at 25 °C for the C_8 proton (▲) and C_2 proton (○). Open figures represent corresponding line widths in the presence of phosphate added as 3′-AMP under the same conditions. The addition of 0.1 M sodium phosphate to 2′,3′-cAMP is shown for the C_2 proton (□) and the C_8 proton (◇).

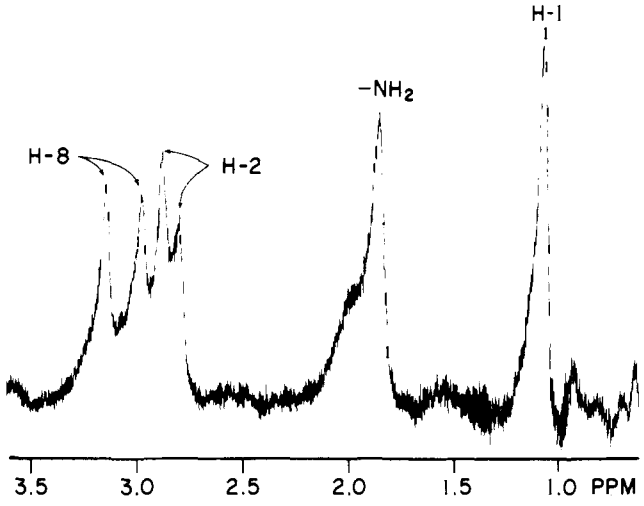

Figure 4. 360-MHz ^{1}H NMR spectrum of cyclic adenylate-methylmercury mixture. Spectrum was obtained at 3 ± 2 °C, pH 6.2, for a solution of 0.14 M 2′,3′-cAMP and 0.18 M CH_3HgOH. Resonance assignments are described in text, and are tentative for H_8 and H_2.

Scheme I

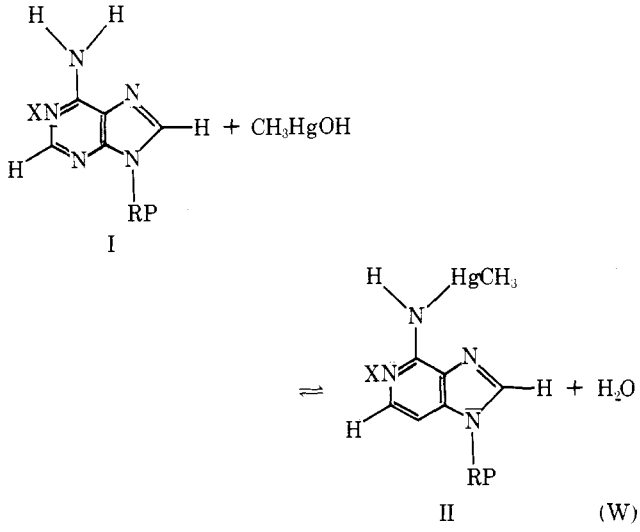

signal. The amino resonances for the mercurated and nonmercurated species are resolved completely at higher temperatures and lower pH, because of a selective upfield shift of the smaller, broad resonance (Figure 5).

The origin of the resolved amino resonances in Figure 5 can be assigned from consideration of the overall species distributions shown in Figure 2 as a function of pH. All species of nucleotide can be segregated into two groups: the free amino species (HA, MA, and A, designated as group I) and the amino mercurated species (HAM, MAM, and AM, group II). Because rapid interaction is expected for both the proton and for CH_3Hg^+ at the N_1 site, the resolution into two NMR species must arise from slow exchange only between the free amino and the aminomercurated species. This assignment is supported by the agreement between the sum of the free amino and of the mercurated amino species (Figure 2) with the areas of the downfield (2 protons) and upfield (1 proton) low pH resonances, respectively (Figures 5A,B). It is noteworthy that the species HAM, the aminomercurated nucleotide protonated at N-1, has been overlooked by previous authors. The necessity of including this species is argued below (see Discussion). The formation constant for HAM is listed with those of the other species in Table II. The reaction of aminomercuration is viewed as shown in Scheme I, where I and II provide the low pH downfield and upfield amino resonances, respectively. Each is defined as mixtures of rapidly interchanging N_1-protonated (X = H^+), N_1-mercurated (X = CH_3Hg^+), and free N_1 ligand (X = no reactant). Thus, the resonance corresponding to I is a coalesced result of the separate resonances of MA, HA, and A (Figure 2) in fast exchange, whose line width in the absence of slow exchange is a weighted average of the individual contributions of these species:

$$\pi W_1 = \frac{P_{MA}}{T'_{2MA}} + \frac{P_{HA}}{T'_{2HA}} + \frac{P_A}{T'_{2A}}$$

where P is the mole fraction of a given species and T'_2 is the overall transverse relaxation time:

$$\frac{1}{T'_2} = \frac{1}{T_2} + \frac{1}{T^*_2}$$

where T^*_2 represents lifetime exchange broadening factors that add to the natural line width defined by $1/T_2$. The latter includes field inhomogeneity and intrinsic transverse relaxation. Similarly, the line width of II is established by rapid exchange between AM, MAM, and HAM (Figure 2). Analogous weighted averages in terms of chemical shifts establish the spectral positions of I and II at any pH. With this definition, the overall reaction can be treated as a two-site exchange problem for the amino and C_8 and C_2 protons and a three-site problem (I, II, and H_2O) for the amino protons. The latter contains the kinetic restriction that the rate of change of magnetization of II and H_2O can contribute to that of I, but not to that of each other. The Bloch equations modified for exchange[21] were extended to a three-site problem with this restriction (see Appendix). This approach provided for the iteration of τ values to produce the calculated spectra shown in Figures 5A–C for the C_2, C_8, and amino proton resonances.

The calculated $-NH_2$ spectra (Figure 5) were obtained without direct measurement of the required chemical shifts for I, II, and W at the zero exchange condition.[22] At the lower pH values the observed resonances are quite close to their zero exchange shifts. Accordingly, the three-site calculation produces a line shape for I and II that is unaffected by considerable changes in the value of $(\delta_I - \delta_W)$. This renders the determination of $(\delta_I - \delta_{II})$ at zero exchange unambiguous for lifetimes that correspond to the observed line shapes at both 360 and 100 MHz. For the latter field frequency the line widths of the calculated I and II (coalesced) resonances correspond favorably with that of the observed signals (Figure 1) for the three pH values of Figure 5. This shows that the pH profile for line broadening at 100 MHz is defined mainly by the zero exchange chemical shifts, rather than by the lifetimes themselves. The lifetimes are similar for the pH values used (Table I).

Values of τ_I in Table I are obtained from a fitted lifetime:

$$\frac{1}{\tau'_I} = \frac{1}{\tau_I} + k_{Hx}$$

where k_{Hx} (eq 1) represents a small significant correction only at pH 3.7. Lifetimes obtained from the three-site calculations were applied to a two-site system for the C_2 and C_8 protons at 360 MHz. The fitted value of $(\delta_I - \delta_{II})$ for these ring hydrogens is consistent with the observed 100-MHz line widths and approximately to the observed low-temperature frequency separations shown in Figure 4. Although too small to measure accurately, the broadening of the CH_3HgOH methyl protons (not shown) describes the same pH maximum seen, in Figure 3, in conformance with the aminomercuration reaction described by the kinetic parameters listed in Table I.

At pH 6.6 the magnitude of $(\delta_I - \delta_{II})$ is not derived from

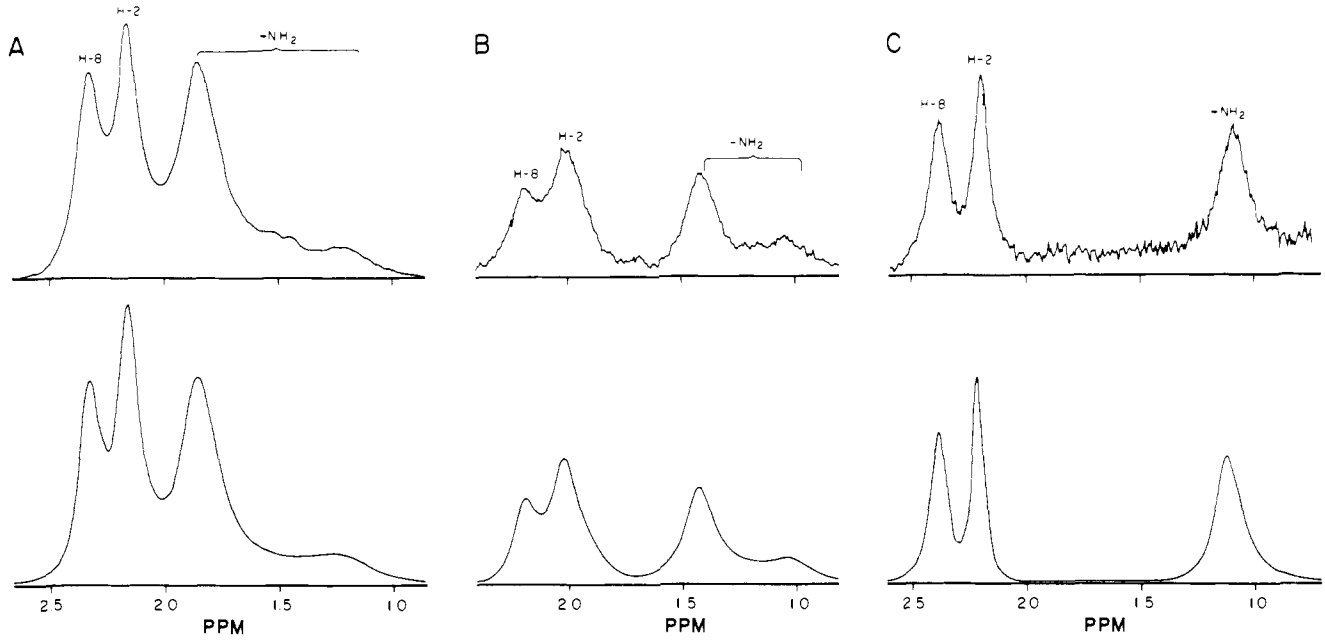

Figure 5. 360-MHz ^{1}H NMR spectra of cyclic adenylate-methylmercury mixtures. Experimental spectra were obtained at pH 3.7 (A), 4.7 (B), and 6.6 (C) at 25 °C for 0.14 M 2′,3′-cAMP and 0.18 M CH_3HgOH. Calculated spectra shown below each experimental curve were obtained from the kinetic and equilibrium values of Tables I and II for a three-site exchange problem (see text, Appendix).

Table I. Kinetic Parameters for Aminomercuration of 2′,3′-cAMP[a]

kinetic parameter	obsd resonance	pH 3.7	pH 4.7	pH 6.6
τ_I,[b] s	$-NH_2$, H_2, H_8	0.012	0.008	0.008
τ_{II}, s	$-NH_2$, H_2, H_8	0.004	0.006	0.009
τ_{HX},[c] s	$-NH_2$	0.011	0.043	1.16
$(\delta_{II} - \delta_I)_{obsd}$, ppm	$-NH_2$	0.610	0.375	0
$(\delta_{II} - \delta_I)_{O\ exch}$, ppm	$-NH_2$	0.719	0.424	0.138
$(\delta_W - \delta_I)_{obsd}$, ppm	$-NH_2$	2.94	2.62	2.00
$(\delta_W - \delta_I)_{O\ exch}$, ppm	$-NH_2$	3.05	2.75	2.14
$(\delta_{II} - \delta_I)_{O\ exch}$	H_2	0.267	0.224	0.141
$(\delta_{II} - \delta_I)_{O\ exch}$	H_8	0.309	0.258	0.171
W_{calcd} (3), 100 MHz[d]	$-NH_2$	56	52	26
P_I (3)[e]	$-NH_2$	0.000 97	0.000 83	0.000 61
P_{II} (3)	$-NH_2$	0.000 31	0.000 45	0.000 67
P_I (2)	H_2, H_8	0.76	0.65	0.48
P_{II} (2)	H_2, H_8	0.24	0.35	0.52

[a] Parameters used for 360-MHz line-shape calculations of Figure 5. Data were obtained at 28 °C, 0.18 M CH_3HgOH, and 0.14 M 2′,3′-cAMP. [b] τ_I for NH_2 is the lifetime of *each* amino proton. The total amino proton lifetime is $\tau_I/2$ from the relation $\tau = (\tau_a\tau_b)/(\tau_a + \tau_b)$, where $\tau_a = \tau_b$. [c] τ_{HX} is the reciprocal of k_{HX} obtained from eq 1, where $k_B = 50\ M^{-1}\ s^{-1}$ and B = H_2O. [d] The numbers in parentheses indicate the number of exchange sites used in the calculation. For three-site exchanges all T_2 values = 0.03 s, due to instrumental broadening for these particular 360-MHz experiments. T_2 values at 100 MHz = 0.2 (C_8), 0.3 (C_2), and 0.07 ($-NH_2$), taken from zero exchange conditions. [e] Calculated line widths of the coalesced I and II resonances at 100 MHz (three-site calculations).

comparison of the I and II resonances, which are coalesced at both 360 and 100 MHz. The observed line width (W_{obsd}) contains a field-independent and field-dependent component:

$$W_{obsd} = \frac{1}{\pi T_2} + W_S + W_F$$

Table II. Association Constants (25°C) for CH_3Hg^{II}-Nucleotide Binding

	reaction	log (formation constant)	ref
(1)	$CH_3Hg^+ + OH^- \rightleftharpoons CH_3HgOH$	9.41	7
(2)	$CH_3Hg^+ + CH_3HgOH \rightleftharpoons (CH_3Hg)_2{}^+OH$	2.37	7
(3)	$cAMP^a + H^+ \rightleftharpoons cAMPH^+$ (N_1)	3.55	4
(4)	$cAMP + CH_3Hg^+ \rightleftharpoons cAMPHgCH_3{}^+$ (N_1)	3.0	8
(5)	$cAMP + CH_3HgOH \rightleftharpoons cAMPH_{-1}HgCH_3 + H_2O$ (C_6NH_2)	1.1	8
(6)	$cAMPHgCH_3{}^+(N_1) + CH_3HgOH \rightleftharpoons cAMPH_{-1}(HgCH_3)_2{}^+ + H_2O$ (N_1, C_6NH_2)	1.9	8
(7)	$cAMPH_{-1}HgCH_3(C_6NH_2) + H^+ \rightleftharpoons cAMPH^+H_{-1}HgCH_3$ (N_1, C_6NH_2)	3.6	b
(8)	$cGMPH_{-1}{}^- + H^+ \rightleftharpoons Guo\ (N_1)$	9.24	13
(9)	$cGMP + H^+ \rightleftharpoons cGMPH^+$ (N_7)	2.23	13
(10)	$cGMPH_{-1}{}^- + CH_3Hg^+ \rightleftharpoons cGMPH_{-1}HgCH_3$ (N_1)	8.1	8
(11)	$cGMP + CH_3Hg^+ \rightleftharpoons cGMPHgCH_3{}^+$ (N_7)	4.5	8
(12)	$cGMPH_{-1}HgCH_3$ (N_1) $+ CH_3Hg^+ \rightleftharpoons cGMPH_{-1}(HgCH_3)_2{}^+$ (N_1, N_7)	4.5	8
(13)	$cGMPH_{-1}(HgCH_3)_2{}^+$ (N_1,N_7) $+ CH_3HgOH \rightleftharpoons cGMPH_{-1}(HgCH_3)_3{}^+ + H_2O$ (N_1, N_7, C_2NH_2)	0.8	8
(14)	$1\text{-}MeAdoH_{-1} + H^+ \rightleftharpoons 1\text{-}MeAdo$ (C_6NH_2)	8.55	b
(15)	$1\text{-}MeAdo + CH_3HgOH \rightleftharpoons 1\text{-}MeAdoH_{-1}HgCH_3 + H_2O$ (C_6NH_2)	3.2	b

[a] cAMP and cGMP refer to the 2′,3′-cyclic monophosphates of adenosine and guanosine, respectively. [b] Constants determined in this work. $K_W = 10^{-14}$ for conversion of literature constants to the forms used.

Because of the independence of line shape and $(\delta_I - \delta_W)$ and the fact that II cannot exchange with W in Scheme I, the

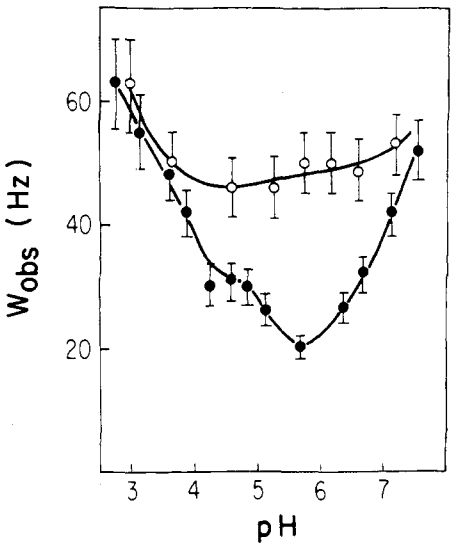

Figure 6. Amino ^{1}H NMR line width vs. pH for adenylate-methylmercury-phosphate mixtures. Spectra were obtained at 100 MHz, 25 ± 2°C for 0.14 M CH_3HgOH in solutions of 0.14 M 2′,3′-cAMP (closed circles) and 0.14 M 3′-AMP (open circles).

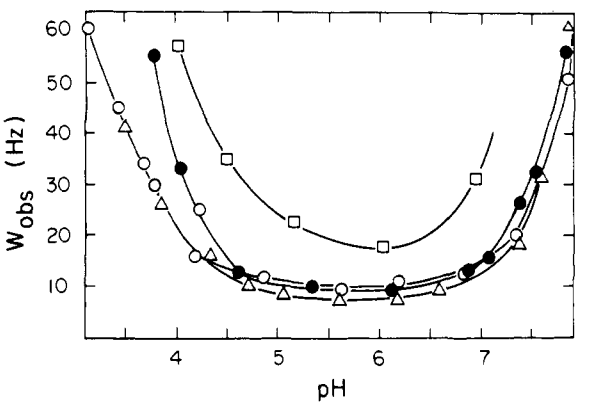

Figure 7. Amino ^{1}H NMR line width vs. pH of guanylate–methylmercury mixtures. Spectra were obtained at 100 MHz at 25 °C from 0.14 M 2′,3′-cGMP and methylmercury hydroxide concentrations of 0 (○), 0.05 (△), 0.15 (●), and 0.3 M (□).

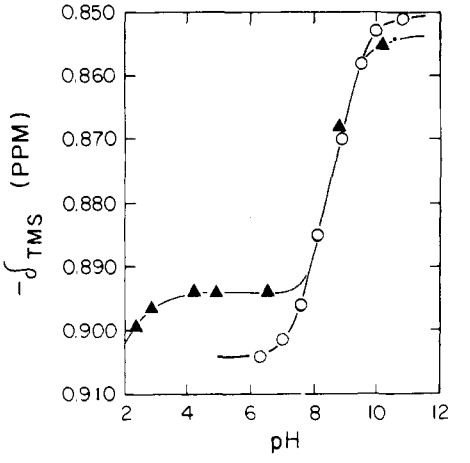

Figure 8. pH dependence of chemical shift of the purine ring proton resonances of 1-methyladenosine. The chemical shifts for the superimposed resonances of the C_2 and C_8 protons of 0.097 M 1-methyladenosine in the presence of 0.0438 M methylmercury (closed circles) and of the C_2 proton resonance of 0.03 M 1-methyladenosine (open circles) were obtained at 100 MHz with a Me_4Si capillary reference at 25 °C.

field-independent broadening (W_S) represents slow lifetime exchange between I and W, while the field-dependent component (W_F) is frequency-dependent broadening for I and II in fast exchange. The W_F term is well approximated by $W_F = 4\pi P_I^2 P_{II}^2(\delta_I - \delta_{II})^2(\tau_I + \tau_{II})$, where P, the mole fractions, and τ, the lifetimes, are the same at 100 and 360 MHz. The shift term (ppm × field frequency) is used to determine both the field-dependent broadening at 100 MHz and W_S, which is the same at both frequencies:

$$W_{obsd(360MHz)} - W_{obsd(100MHz)} = [(3.6)^2 W_{F(100MHz)}] - W_{F(100MHz)}$$

At 100 MHz W_F is small (<2 Hz) for a field dependence of 20 Hz, which leaves the major portion of the line width, 20 Hz as W_S, the lifetime broadening for I → W exchange. The value, $\tau_S = 1/\pi W_W = 0.016$ s, is *twice* the value of τ_I, owing to the ½ probability that the amino proton will go to the water site (see Appendix). The value $\tau_I = 0.008$ s^{-1} is used to obtain $(\delta_I - \delta_{II})$ for the calculated line shape for all protons at 360 MHz and the I → II line width at 100 MHz (Table I).

Phosphate was added to the methylmercury–nucleotide mixture in order to further assess the contribution of exchange routes between $-NH_2$ and H_2O other than Scheme I. Phosphate acts as an amino proton acceptor as B in eq 1.[2,5,6] Under specific pH conditions the phosphate–methylmercury interaction is of minimal significance in establishing the overall binding equilibria.[14] The addition of phosphate produces two concomitant effects: a broadening of the amino proton resonance (Figure 6) and a sharpening of the C_2 and C_8 resonances (Figure 3). This further supports aminomercuration as the sole line-broadening factor for the amino protons in H_2O exchange.

The effect of methylmercury on the $-NH_2$ line width of guanine is shown in Figure 7. Although the mercury–guanine N_7 binding constant is greater than that of the adenine N_1,[8] no broadening is observed for guanine at mercury concentrations that produce pronounced broadening for adenine (Figure 7). The low pH line sharpening that occurs in the presence of CH_3HgOH (Figure 7) is once again a reflection of decreased $NH_2 \rightarrow H_2O$ exchange, due to the mercury–proton competition for the guanine N_7 site. The chief difference between the guanine and adenine systems under these conditions is the insignificantly low concentration of the aminomercurated form in the case of guanine. The unchanged line shape for the guanine amino would reflect a low rate of direct aminomercuration associated with the low concentration of II (in analogy to II of adenine). This is borne out by the appearance of line broadening at a $[CH_3HgOH]/[2',3'\text{-cGMP}]$ ratio high enough to produce a significant concentration of this species (Figure 7). In the low pH range this higher ratio (~2) represents little change in the mole fraction of the N_7-mercurated guanine, which approaches a value of 1 at the lower ratios. Again, this demonstrates that aminomercuration is the major broadening mechanism, rather than amino-to-water exchange per se from the N_7-mercurated purine.

The direct relation between aminomercuration and $-NH_2$ resonance line broadening is demonstrated further by the addition of CH_3HgOH to solutions of 1-methyladenosine. The N_1-methyl nucleobase differs markedly from the unsubstituted purine in the inaccessibility of N_1 for binding and the much greater acidity of the amino group. The acid dissociation constant for the reaction $-NH_2 \rightleftharpoons -NH^- + H^+$, determined from the pH dependence of the C_2 proton chemical shift, is 8.55 (Figure 8). Accordingly, the pH dependence of lifetime broadening for the $-NH_2$ protons above pH 4 is described by a rate constant for hydroxyl ion catalysis, $k_{OH} = 2.4 \times 10^{11}$ M^{-1} s^{-1} (Figure 9). This value is typical of those determined for "normal" acids titratable in aqueous solution[24] and is about four orders of magnitude greater than that of the unsubstituted

nucleobase.[2] As expected, mercuration of the amino of 1-methyladenosine is virtually quantitative, as shown by the pH-independent chemical shift values between pH 4 and 7 (Figure 8). A CH_3Hg^{II} to NH_2 binding constant, $K_{AM} = 10^{3.2}$, is extracted from the low pH data for the methylmercury nucleoside mixtures and from limiting chemical shifts of 0.855 and 0.904 ppm (Me_4Si) for the mercurated and free amino, respectively. Since binding is virtually complete, the broadening observed with the addition of methylmercuric hydroxide to 1-methyladenosine (Figure 9)[25] can arise only from exchange reactions linked directly to aminomercuration, rather than from separate reactions involving $-NH_2$ to H_2O exchange. A close comparison of experimental resonance areas and areas expected for quantitative mercury binding to the amino group further demonstrates that the nucleobase sites other than the amino do not compete as ligands.[9] This is further supported by the independence of C_2 and C_8 and methylmercury CH_3 proton chemical shifts as a function of pH for 1-methyladenosine–methylmercury mixtures, in which CH_3HgOH is in sufficient molar excess to preclude significant concentrations of free nucleoside (data not shown).

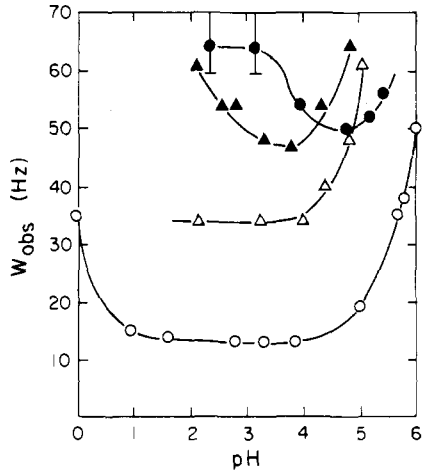

Figure 9. Amino ^1H NMR line width vs. pH of 1-methyladenosine. Spectra at 100 MHz were obtained at 25 ± 2 °C: (○) 0.15 M M^1-ado, 6.7 M $NaClO_4$; (△) 0.15 M M^1-ado; (●) 0.098 M M^1-ado, 6.7 M $NaClO_4$, 0.029 M CH_3HgOH; (▲) 0.14 M M^1-ado, 0.16 M CH_3HgOH. The use of $NaClO_4$ is explained in footnote 25.

Discussion

Mercuration of the adenine amino is a relatively slow equilibrium reaction with pseudo-first-order rate constants in the vicinity of 10^2 s^{-1}. These slow rates are consistent with the well-established difficulty of proton transfer from the nucleotide amino group.[2] The effects of this reaction on NMR line shapes are accounted for by treating the free amino and mercurated amino forms as ensembles of rapidly interacting species.

Several lines of evidence demonstrate the close connection between the aminomercuration reaction and $-NH_2$ to H_2O exchange measured by the $-NH_2$ line width at two field frequencies. This leads to the conclusion that reactions of the type expressed by eq 1 do not contribute to the line shape of the amino resonance, with the N-1 mercurated form as a proton donor. The (N-1)-protonated nucleotide makes a small contribution, owing to the low value of PHA. This leads to a small correction in T_N only at pH 3.7. Mercuration of N-1 does not produce the great increase in amino acidity that is observed with N-1 protonation. This is further supported by the decrease in $-NH_2$ line width for both adenosine and guanosine monophosphates upon CH_3HgOH addition. Apparently, the inductive effect of CH_3Hg^+ is much less than that of the proton at the N-1 site, owing to the lower charge density of the methylmercury cation. This leads to a number of conclusions regarding the reactivity of certain key species. First, the $-NH^-$ form of the amino is excluded as an intermediate in aminomercuration of the N-1 mercurated nucleotide (MA). The aminomercuration reaction can be viewed as a concerted reaction for CH_3HgOH binding and water elimination involving a four-center hydrogen-bonded intermediate of the type shown.

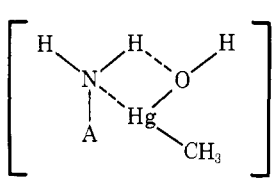

Second, the amino protons of any of the species making up II should be less acidic than their counterparts in I, i.e., $\tau_{(II \rightarrow W)} \gg \tau_{(I \rightarrow W)}$ for catalysts other than methylmercury. Third, CH_3Hg^+ should have a lower affinity than H^+ for the amino group, providing for increased rates for aminomercuration equilibria in the presence of phosphate:

$$-NHHgCH_3 + HPO_4^{2-} \rightleftharpoons -NH^- + CH_3HgHPO_4^-$$

This accounts for the phosphate broadening of the amino resonance in the presence of methylmercury.

Within a wide range of exchange parameters used for generating line shapes a unique set of species distribution is required to fit simultaneously all three 360-MHz spectra obtained at three different pH values. It is clear that the use of the literature association constants for the calculation of these distributions will not provide this fit unless a ninth equilibrium species, HAM, is considered with a formation constant of $10^{3.3}$–$10^{3.6}$. To ignore this species, as others have done,[8,10] would require a twofold adjustment in all formation constants required for the generation of the observed line shapes (Figure 5). Use of the literature constants and inclusion of this species are the preferred alternatives. There is no a priori consideration against the existence of HAM and the fitted formation constant is quite close to the formation constant for the analogous species, HA, which is expected from the above considerations regarding the relative charge densities of CH_3Hg^+ vs. the proton (see above). The species HAM exhibits a maximum at the same pH as does MA (Figure 2). This would explain why the existence of HAM might not be seen by Raman techniques.[10] Also, its concentration would be very small under the dilute conditions used for studying methylmercury–nucleotide equilibria by spectrophotometric means.[8] Its effect at higher nucleotide–CH_3HgOH concentrations is expressed in the ratio of P_I/P_{II}. With this species addition the required ratio of 1.4 is met quite closely at pH 4.7, while calculations excluding HAM produce a $P_I/P_{II} = 2.5$. In the latter case the signal assigned to II at pH 4.7 would not be visible (Figure 5). Finally, literature constants for the formation of CH_3Hg^+, $(CH_3Hg)_2{}^+OH$, and CH_3HgOH[7,15] provide adequate fits of our own data on the pH dependence of the methylmercury $-CH_3$ proton chemical shift, which argues against large adjustments in the formation constants determined by others.

Lifetimes for aminomercuration are established not only by the forward reaction of Scheme I, but also by reactions promoting demercuration such as the phosphate reaction described above. Direct protonation of the mercurated amino is another possibility. The relative contributions of these reactions would require assessment of the reactivities of each of the six nucleotide forms. The required spectral parameters of each species may be accessible with the use of sufficiently high magnetic fields used in conjunction with kinetic analysis of amino proton exchange.

Appendix

Line-Shape Calculation for CH_3HgOH Catalysis of Amino Proton Exchange. Derivation of a secular expression for the exchange of magnetization of the amino protons from the reaction of Scheme I begins with consideration of two equally possible destinations for each proton.

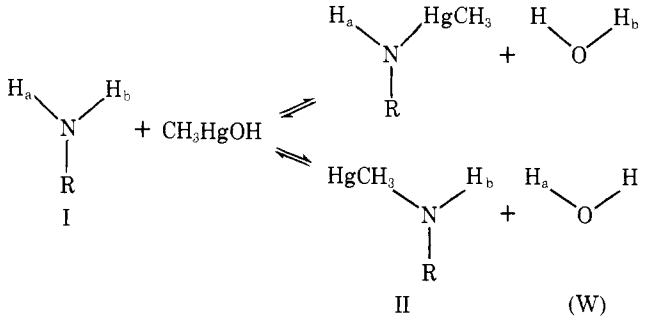

Following the procedures and definitions presented by McConnell,[21] the rate of change of magnetization for each amino proton can be written separately. The rate of change of out-of-phase magnetization of H_a on I (Ia) is written as two separate reactions with a probability of 0.5:

$$\frac{dv_{(1a)}}{dt} = 0.5\left(\Delta\omega_{(1a)}u_{(1a)} - \frac{v_{(1a)}}{\tau_{2(1a)}} + \frac{v_{(11a)}}{\tau_{(11a)}} - \omega_1 M_z{}^a\right) + 0.5\left(\Delta\omega_{(1a)}u_{(1a)} - \frac{v_{(1a)}}{\tau_{2(1a)}} + \frac{v_{(Wa)}}{\tau_{(Wa)}} - \omega_1 M_z{}^a\right)$$

where $\Delta\omega_{1a}(\text{rad})s^{-1} = (\omega_{(1a)} - \omega)$, $u_{(1a)}$ is the in-phase magnetization, $v_{(1a)}$ is the out-of-phase magnetization, τ is the lifetime, and $1/\tau_2 = 1/T_2 + 1/\tau$. The Ho magnetization is $M_z{}^a = P_1$, where P_1 is the mole fraction of I as defined in the text.

Similarly, $dv_{(1b)}/dt$ is obtained and combined with $dv_{(1a)}/dt$ according to the following relationships:

$$v_1 = v_{(1a)} + v_{(1b)},\ v_{11} = \frac{v_{(11a)} + v_{(1b)}}{2}$$

$$v_W = \frac{v_{(Wa)} + v_{(Wb)}}{2}$$

(the second water proton is ignored, as it does not participate in the reaction, while both H_a and H_b exchange magnetization with II and W in each half-reaction). Although

$$\tau_{a,b} = \frac{\tau_{(1a)}}{2} = \frac{\tau_{(1b)}}{2}$$

from the relation

$$\frac{1}{\tau_{a,b}} = \frac{1}{\tau_{(1a)}} + \frac{1}{\tau_{(1b)}}$$

for simplicity we define $\tau_1 = \tau_{(1a)} = \tau_{(1b)}$ where $\tau_{(1a)} = \tau_{(1b)}$ and $\Delta\omega_{(1a)} = \Delta\omega_{(1b)} = \Delta\omega_{(1)}$ in this particular case, due to rapid rotation. Because of the large, rapidly exchanging reservoir of water, $\tau_{(Wa)} = \tau_{(Wb)} = \tau_W$. Also, $\tau_{(11a)} = \tau_{(11b)} = \tau_{11}$. The combination gives

$$\frac{dv_1}{dt} = \Delta\omega_1 u_1 - \frac{v_1}{\tau_{21}} + \frac{v_{11}}{\tau_{11}} + \frac{v_W}{\tau_W} - 2P_1$$

where the instrumental constant ($\omega_1 = \gamma H_1$) is set equal to 1.

A corresponding expression for the u magnetization

$$\frac{du_1}{dt} = -\Delta\omega_1 v_1 - \frac{u_1}{\tau_{21}} + \frac{u_{11}}{\tau_{11}} + \frac{u_W}{\tau_W}$$

is combined with dv_1/dt according to the relation $G_1 = (u + iv)$ to give the rate expression for species I:

$$-G_1\left(\frac{1}{\tau_{21}} + i\Delta\omega_1\right) + \frac{G_{11}}{\tau_{11}} + \frac{G_W}{\tau_W} = 2iP_1$$

Expressions for II and W are obtained in the same way to give

$$-G_{11}\left(\frac{1}{\tau_{211}} + i\Delta\omega_{11}\right) + \frac{G_1}{2\tau_1} = iP_{11}$$

$$-G_W\left(\frac{1}{\tau_{2W}} + i\Delta\omega_W\right) + \frac{G_1}{2\tau_1} = iP_W$$

where $\Delta\omega_{11a} = \Delta\omega_{11b} = \Delta\omega_{11}$ and $\Delta\omega_{(Wa)} = \Delta\omega_{(Wb)} = \Delta\omega_W$.

The W and II terms are missing from the II and W expressions, respectively, owing to the fact that II and W do not exchange magnetization directly in the reaction. Also, it is noteworthy that the lifetime of II and W in their corresponding equations corresponds to $2\tau_1$ in the slow exchange limit, which reflects the competition of I and W for a given $-NH_2$ proton.

The canonical forms are obtained by the method of determinants. These are added to give the complex expression, from which the imaginary part is separated by using the complex conjugate of the denominator. An APL computer program for the imaginary part is available on request. Frequencies in hertz are multiplied by 2π for conversion to radians.

For calculation of the mole fraction, [I] = AT (PA + PHA + PMA), [II] = AT (PAM + PMAM + PHAM), and [W] = 2 × 55, where AT is the total nucleotide concentration and the terms within the parentheses are defined in the text (Figure 2). Although [W] is multiplied by 2 to account for the second water proton, [I] is not, since this correction is implicit in the derivation.

All lifetimes are related by

$$\frac{\tau_1}{P_1} = \frac{\tau_{11}}{P_{11}} = \frac{\tau_W}{P_W}$$

References and Notes

(1) This work was performed in partial fulfillment of requirements for a Ph.D. in Biophysics by D-L.H. and was supported by National Science Foundation Grants BMS-74-24311 and PCM-77-20154.
(2) B. McConnell and P. C. Seawell, *Biochemistry*, **11**, 4382 (1972).
(3) B. McConnell and P. C. Seawell, *Biochemistry*, **12**, 4426 (1973).
(4) B. McConnell, *Biochemistry*, **13**, 4516 (1974).
(5) D. G. Cross, A. Brown, and H. F. Fisher, *Biochemistry*, **14**, 2747 (1975).
(6) B. McConnell, *Biochemistry*, **17**, 3168 (1978).
(7) G. Schwarzenbach and M. Schellenberg, *Helv. Chim. Acta*, **48**, 28 (1965).
(8) R. B. Simpson, *J. Am. Chem. Soc.*, **86**, 2059 (1964).
(9) S. Mansy, T. E. Wood, J. C. Sprowles, and R. S. Tobias, *J. Am. Chem. Soc.*, **96**, 1762 (1974).
(10) S. Mansy and R. S. Tobias, *J. Am. Chem. Soc.*, **96**, 6874 (1974).
(11) S. Mansy and R. S. Tobias, *J. Chem. Soc., Chem. Commun.*, 957 (1974).
(12) S. Mansy and R. S. Tobias, *Biochemistry*, **14**, 2952 (1975).
(13) S. Mansy and R. S. Tobias, *Inorg. Chem.*, **14**, 287 (1975).
(14) S. Mansy, J. P. Frick and R. S. Tobias, *Biochim. Biophys. Acta*, **378**, 319 (1975).
(15) S. Libich and D. L. Rabenstein, *Anal. Chem.*, **45**, 118 (1973).
(16) D-L. Hoo, C. C. Hu, T. P. Tsai, and C. C. Hsu, *J. Chin. Agric. Chem. Soc.* **10**, 73 (1973).
(17) B. McConnell and P. V. von Hippel, *J. Mol. Biol.*, **50**, 317 (1970).
(18) A. H. J. Maas, *J. Appl. Physiol.*, **30**, 248 (1971).
(19) The Bruker HXS-360 NMR spectrometer is part of a National Facility funded by National Science Foundation Grant GR 23633 and National Institutes of Health Grant RR 00711.
(20) Proton transfer, k_B (eq 1), is a function of ($pK_B = pK_{-NH_2}$), the difference in acid dissociation constants of the acceptor B and $-NH_2$ of the N_1-mercurated, N_1-protonated, or free ligand, when $pK_B < pK_{-NH_2}$.[24]
(21) H. M. McConnell, *J. Chem. Phys.*, **26**, 430 (1958).
(22) The zero exchange chemical shifts for each species follow the order $\delta_{H_2O} > \delta_{AM} > \delta_{MAM} > \delta_{HAM} > \delta_{MA} > \delta_{HA}$ with respect to an upfield reference. Although these values can be determined at an appropriate pH, the zero exchange value of $\delta_I = P_{HA}\delta_{HA} + P_{MA}\delta_{MA} + P_A\delta_A$ is inexact owing to the

unknown magnitude of stacking effects as a function of pH.[23] The same difficulty applies to the determination of δ_{II} at zero exchange.

(23) M. P. Schweizer, S. I. Chan, and P. O. P. Ts'o, *J. Am. Chem. Soc.*, **87**, 5241 (1965).
(24) M. Eigen, *Angew. Chem., Int. Ed. Engl.*, **1**, 1 (1964).
(25) The narrowing of the exchange-broadened resonances into the observable range with the addition of ≥6 M $NaClO_4$ is accounted for quantitatively by the decreased concentration and activity of H_2O, which acts as the major proton acceptor catalyst at low pH (Hoo and McConnell, in preparation). The observed broadening with H_2O as acceptor (eq 1) is in agreement with the broadening calculated from eq 1, where $k_B = k_O \times 10^{(pK_{H_2O} - pK_{NH_2})}$, $k_O = 10^{10}$ for water, $pK_{H_2O} = -1.7$, and $pK_{NH_2} = 8.55$.[6]
(26) J. J. Mulvihill, *Science*, **176**, 132 (1972).
(27) D. W. Gruenwedel and N. Davidson, *Biopolymers*, **5**, 847 (1967).

Application of Photoelectron Spectroscopy to Biologically Active Molecules and Their Constituent Parts. 6. Opiate Narcotics[1]

L. Klasinc,* B. Ruščić, A. Sabljić, and N. Trinajstić

Contribution from The Rugjer Bošković Institute, P.O.B. 1016, 41001 Zagreb, Croatia, Yugoslavia. *Received December 26, 1978*

Abstract: The He(I) photoelectron (PE) spectra are reported of the free bases of morphine, codeine, heroin, and methadone. They are assigned by the composite molecular method of Rabalais, using the PE spectra of 2-methoxyphenol, 2-methoxy-4-methylphenol, crotyl alcohol, 3-penten-2-ol, allyl acetate, phenyl acetate, diphenylmethane, and 1,1-diphenylacetone to compare the common details of electron structure. The results indicate that their molecular rather than electronic structure is important for analgesic activity.

Opiate narcotics are substances whose actions are similar to those of morphine (Figure 1). Their principal therapeutic use is in the relief of pain.[2] Methadone, although differing considerably from morphine-like narcotics in its chemical structure (Figure 2), exhibits a comparable analgesic potency.[3] It is believed that the valence molecular orbital structure of opiate narcotics plays an important role in the attempt to rationalize their activity.[4] Energies and electron distributions associated with the valence orbitals influence the way in which narcotics participate in weak bonding interactions with their receptors.[5] The electronic structure of opiate narcotics has been extensively investigated in numerous theoretical studies by semiempirical[6-8] and nonempirical[9] molecular orbital calculations. Experimental data are available only for morphine and nalorphine,[9] whose PE spectra have been recorded, although with poor resolution.

Since the calculated results, even those obtained with the nonempirical methods, match poorly the experimental values (~2-eV difference), we decided to compare the PE spectra of the whole series of opiates, starting with the opiate having the simplest structure, and, in order to assign their spectra, to use an empirical approach with qualitative molecular orbital interactions known as the composite molecular approach.[10] The interpretation is simplified by partitioning the complex morphine narcotics into three components: polysubstituted benzene, unsaturated alcohol or ester, and trialkylamine. Only a weak inductive interaction between these components is assumed. The same procedure was used for methadone with the components diphenylmethane, acetone, and trialkylamine.

Experimental Section

Gas-phase He(I) PE spectra were measured with a Vacuum Generators UV-G3 spectrometer.[11] The following compounds were investigated: free bases of morphine, codeine, heroin, and methadone, 2-methoxyphenol, 2-methoxy-4-methylphenol, crotyl alcohol, 3-penten-2-ol, allyl acetate, phenyl acetate, diphenylmethane, and 1,1-diphenylacetone. The PE spectra were measured at room or elevated temperature (morphine, codeine, and heroin at 230 °C, methadone at 120 °C) in the inlet system. Low resolution (30–50 meV) for the complete spectra and high resolution (~15 meV) with an expanded scale for individual systems were used. The energy scale was calibrated using $^2P_{3/2}$ and $^2P_{1/2}$ lines of Xe and Ar. All compounds investigated were of high purity and had been redistilled or recrystallized before use.

Results and Discussion

The spectra of the compounds investigated are shown in Figures 3–6. The vertical ionization energies, defined for the highest peak in a system, are listed above the spectrum. Less certain values are given to one decimal place.

Morphine. The main subunit in the morphine molecule is a polysubstituted benzene. In benzene, the occupied π orbitals, a_{2u} and e_{1g}, give rise in the PE spectrum to systems at 12.35 and 9.23 eV, respectively.[12]

Upon monosubstitution the degeneracy of the e_{1g} benzene orbitals is lifted.[13] In phenol (C_{2v} symmetry assumed), the a_2 component of the e_{1g} benzene orbital does not, for symmetry reasons, interact with the 2p lone pair on oxygen, n_O, and remains at approximately the same energy (9.28 eV) as in benzene. However, the b_1 component is destabilized through antibonding interaction with the n_O orbital (8.56 eV), Figure 7. The remaining two π orbitals in phenol (both of b_1 symmetry) have energies of 11.60 and 13.49 eV.[13b] The first contains mainly an oxygen lone-pair component, while the other corresponds to a stabilized a_{2u} benzene orbital. A similar reasoning attributes to π ionizations the following systems in the PE spectrum of 2-methoxyphenol (Figure 4): 8.13 (π_5), 9.03 (π_4), 11.12 (π_3), 12.5 (π_2), and approximately 14.0 eV (π_1). The top two orbitals can be viewed as antibonding combinations of the components of the benzene e_{1g} orbital with the oxygen lone pairs (Figure 7). Owing to the very low symmetry of the molecule (C_s, at best), the relative ordering of these two orbitals is difficult to infer, but this is not critical. The π_3 and π_2 orbitals are predominantly the negative and positive combinations of the oxygen lone pairs, respectively, while π_1 again corresponds to the a_{2u} benzene orbital. In 2-methoxy-4-methylphenol (Figure 4), introduction of a methyl group at the benzene ring inductively destabilizes the π orbitals relative to 2-methoxyphenol. The destabilizations observed for the top

0002-7863/79/1501-7477$01.00/0